DEPARTMENT OF MATHEMATICS

Coarsening Kinetics from a Variable Mobility Cahn-Hilliard Equation - Application of Semi-implicit Fourier Spectral Method

by J. Zhu, L. Q. Chen, Jie Shen and V. Tikare

REPORT NO. AM211 October 1999

Coarsening Kinetics from a Variable Mobility Cahn-Hilliard Equation - Application of Semi-implicit Fourier Spectral Method

J. Zhu, L. Q. Chen
Department of Materials Science and Engineering
Penn State University, PA 16802, USA

Jie Shen
Department of Mathematics
Penn State University, PA 16802, USA

V. Tikare
Materials Modeling and Simulation
Sandia National Laboratory
Albuquerque, NM 87185-1411

October 7, 1999

Abstract

An efficient Semi-Implicit Fourier-Spectral method is implemented to solve the Cahn-Hilliard equation with a variable mobility. The method is orders of magnitude more efficient than the conventional forward Euler finite-difference method, thus allowing us to simulate large systems for longer times. We studied the coarsening kinetics of interconnected two-phase mixtures using a Cahn-Hilliard equation with its mobility depending on local compositions. In particular, we compared the kinetics of bulk-diffusion- and interface-diffusion-dominated coarsening in two-phase systems. Results are compared with existing theories and previous computer simulations.

1 Introduction

The diffuse-interface phase-field approach is emerging as a powerful mathematical model for simulating the mesoscale morphological pattern formation and interface motion, see, for example, [9] for a brief overview, and the references therein. It usually involves the numerical solution of a time-dependent Ginzburg-Landau equation (TDGL), or a Cahn-Hilliard equation (CH), or systems of TDGLs and/or CH equations. For example, a single CH equation has been extensively applied to modeling coarsening kinetics of two-phase microstructures. Microstructural instability as a result of coarsening is of a major concern for many structural materials since the mechanical properties of a material usually degrade as the microstructure coarsens. Within the phase-field context, the composition field, or more precisely, the compositional deviation from the overall average composition, acts as a phase field in an isostructural two-phase system.

There have been many existing simulations using a CH equation employing a constant mobility, corresponding to bulk-diffusion-dominated coarsening [2, 3, 4]. It is generally agreed that during late stages of coarsening two-phase microstructures exhibit dynamical scaling (or self-similarity), i.e., the morphology at a given time can statistically match that of an earlier time by a global change of scale. Consequently, the growth of the system is characterized by a single length, the average microstructural length scale, to which all other relevant lengths must scale. For the bulk-diffusion-controlled coarsening, the average scale of a two-phase microstructure, $\bar{R}^3$, is found to approximately follow the power law, $\bar{R}^3 - R_o^3 = Kt$, where R_o is the average length at time $t = 0$, and K is the rate constant for coarsening.

However, there have been very few studies of the effect of a variable mobility on the coarsening kinetics of a two-phase system. The direct numerical solution of a Cahn-Hilliard equation with a variable mobility was performed by Lacasta et al. who showed a significant effect of composition dependence of the mobility on the coarsening kinetics of a two-phase mixture [5, 6]. Similar results were obtained by Yeung et al. using a cell dynamics model [7]. More recently, Bray et al. derived a growth law corresponding to the CH equation with variable mobility, in the Lifshitz-Slyozov limit where the minority phase occupies a vanishingly small volume fraction [8].

Most of the existing phase-field simulations employed the explicit forward Euler method in time and finite-difference in space. To maintain the stability and to achieve high accuracy for the solutions, the time step and spatial grid size have to be very small, which seriously limits the system size and time duration of a simulation.

Recently, we implemented an accurate and efficient semi-implicit Fourier-spectral method for solving the time-dependent Ginzburg-Landau equations [9]. Semi-implicit Fourier-Spectral methods have been widely used in the field of fluid dynamics [10]. For the time variable, we employed semi-implicit schemes in which the principal elliptic operator was treated implicitly to reduce the associated stability constraint, while the nonlinear terms were still treated explicitly to avoid the expensive process of solving nonlinear equations at each time step. Thus, at each time step, one solves a constant-coefficient elliptic problem which, in the case of periodic boundary conditions, can be solved efficiently and accurately by the Fourier-spectral method whose convergence rate is exponential (for smooth functions) as opposed to second-order by a usual finite-difference method.

For the fourth-order Cahn-Hilliard equation, explicit finite-difference schemes have an even more severe time step constraint than the second-order TDGL equation. As a result, very small time step sizes have to be employed for small grid sizes. Therefore, even for the case of a constant mobility, it is questionable that the so-called "scaling state" of a microstructure has ever been reached in direct simulations because of the limit on simulation time and system size. The cell-dynamics system (CDS) simulation of coarsening kinetics by Oono et al. [11] does not involve the direct solution of the differential equations.

This paper has two main objectives. One is to propose a semi-implicit Fourier spectral method for solving the Cahn-Hilliard equation. Since preliminary application to the Cahn-Hilliard equation with a constant mobility showed orders of magnitude improvement in efficiency compared to explicit forward Euler method [9], the emphasis here will be on its application to the case with variable coefficient (mobility) in the Cahn-Hilliard equation. The second objective is to study the coarsening kinetics of isostructural two-phase systems using a CH equation with a variable mobility. Specifically, we make comparisons between the bulk-diffusion- and interface-diffusion-controlled dynamics by studying the dynamical scaling features and the growth law of interconnected two-phase microstructures.

2 Cahn-Hilliard Equation

An isostructural two-phase system presents perhaps the simplest possible example of phase-field description of two-phase microstructures. In this case, we need only a single field, the compositional field, $C(\mathbf{r},t)$, to describe the microstructure. Within the bulk of the two phases, the composition field assumes the equilibrium values determined by the phase diagram. Across the interfaces from one phase to another, there is a gradual change in composition.

Since a two-phase microstructure is thermodynamically stable, it will evolve to reduce the total interfacial area and thus the total interfacial energy as a function of time. The ratio of the driving force per atom for coarsening to the thermal energy k_BT is relatively small compared to other processes such as bulk phase transformations. In this case, we can safely apply the linear non-equilibrium thermodynamics according to which the atom flux is linearly proportional to the chemical potential gradient. In the laboratory reference system, the flux equation is given by

$$J = -N_V M \nabla \mu \tag{1}$$

where N_V is the number of atoms per unit volume, M is the mobility given by

$$M = C(1-C)[CM_1 + (1-C)M_2] \tag{2}$$

where M_1 and M_2 are atomic mobilities of species 1 and 2, respectively and C is the composition of species 2. In equation (1), the chemical potential, μ, is actually the chemical potential difference between the two species, i.e.,

$$\mu = \mu_2 - \mu_1 \tag{3}$$

where μ_1 and μ_2 are the atomic chemical potentials of species 1 and 2, respectively. In an inhomogeneous and nonequilibrium system such as a two-phase mixture, C and μ vary in space, and thus C is a local composition field and μ is a local chemical potential field. The temporal evolution of the composition, and thus the microstructural evolution, is described by the diffusion equation,

$$\frac{\partial C}{\partial t} = N_V \nabla \cdot M \nabla \mu \tag{4}$$

where t is time.

In order for the diffusion equation (4) to be able to describe coarsening, the contribution of the interfacial energy to the total free energy must be included in the local chemical potential field μ. In the Cahn-Hilliard diffuse interface theory, the interfacial energy is introduced through the gradient energy terms. The total free energy of an inhomogeneous system is then given by [12]

$$F = \int_V \left[f(C) + \frac{1}{2}\kappa(\nabla C)^2 \right] dV \tag{5}$$

where $f(C)$ is the local free energy density and κ is the gradient energy coefficient which can be related to inter-atomic interaction parameters. The local chemical potential is then given by

$$N_V \mu = \frac{\delta F}{\delta C} = \frac{df}{dC} - \kappa \nabla^2 C \tag{6}$$

where $\frac{\delta F}{\delta C}$ represents a variational derivative. Therefore, the nonlinear temporal evolution equation for the local composition field, (the nonlinearized Cahn-Hilliard equation), becomes

$$\frac{\partial C}{\partial t} = \nabla \cdot M \nabla \left[\frac{df}{dC} - \kappa \nabla^2 C \right] \tag{7}$$

To include the effect of thermal fluctuations, the following stochastic equation was proposed by Cook[13],

$$\frac{\partial C}{\partial t} = \nabla \cdot M \nabla \left[\frac{df}{dC} - \kappa \nabla^2 C \right] + \eta(\mathbf{r}, t) \tag{8}$$

where the noise term $\eta(\mathbf{r},t)$ is a Gaussian random variable satisfying the fluctuation dissipation theorem.

In most of the existing numerical simulations, the mobility, M, in the Cahn-Hilliard-Cook equation is assumed to be independent of concentration field variable. With a double-well potential function for the local free energy density, the Cahn-Hilliard equation with constant mobility can be presented in a scaled form as [2]

$$\frac{\partial C(\mathbf{r},t)}{\partial t} = \nabla^2 \left[-C + C^3 - \kappa\nabla^2 C\right] + \eta(\mathbf{r},t) \tag{9}$$

However, based on equation (2), the mobility, M, should be dependent on the composition field. This dependence might produce quite important changes on the coarsening kinetics. A similar scaled form for the Cahn-Hilliard equation with a variable mobility was presented by Langer et al.[14] and Kitahara and Imada[15]

$$\frac{\partial C(\mathbf{r},t)}{\partial t} = \nabla\cdot(1-aC^2)\nabla[-C + C^3 - \kappa\nabla^2 C] + \eta(\mathbf{r},t) \tag{10}$$

Where a is a positive constant. When $a = 0$, the above modified Cahn-Hilliard-Cook equation has the same form of Cahn-Hilliard-Cook equation with constant mobility, describing the dynamics controlled by bulk diffusion. When a equals to 1, the bulk diffusion is severely reduced, which corresponds to the interface diffusion controlled dynamics, i.e., the coarsening process is mainly due to the diffusion along the interface between the two phases. The value of a is dependent on the temperature for a real system. It should be pointed out that equation (10) is essentially the same as that given in equation (8), but presented in a scaled form. Changing a allows us to investigate the role of bulk and interface diffusion in the coarsening kinetics.

3 Semi-Implicit Fourier-Spectral Method

A high quality numerical study of the Cahn-Hilliard-Cook equation requires enough computer time and memory to get physically meaningful result. First, a large system size is necessary to have good statistics and to minimize the effect of periodicity imposed by periodic boundary conditions. Secondly, in order to understand the scaling behavior of morphological pattern evolution, the system has to evolve long enough to reach the true scaling regime. To simplify the problem, we have not included noise term in our study because it usually took much CPU time for generating the noise term at each time step. In this paper, we implement a semi-implicit Fourier-spectral method for solving the Cahn-Hilliard-Cook equation.

3.1 Cahn-Hilliard Equation with a Constant Mobility

Instead of using a finite-difference approximation, we propose to use a Fourier-spectral approximation to equation (9) by transforming the partial differential equation into a sequence of ordinary differential equations in the Fourier space

$$\frac{\partial \tilde{C}(\mathbf{k},t)}{\partial t} = -k^2\{-C + C^3\}_{\mathbf{k}} - \kappa k^4 \tilde{C}(\mathbf{k},t) \tag{11}$$

where $\mathbf{k} = (k_1, k_2)$ is a vector in the Fourier space, $k = \sqrt{k_1^2 + k_2^2}$ is the magnitude of $\mathbf{k}$, $C(\tilde{\mathbf{k}},t)$ and $\{-C+C^3\}_{\mathbf{k}}$ represent the Fourier transform of $C(\mathbf{r}$,t) and the bulk driving force term $-C+C^3$, respectively.

The explicit Euler Fourier-spectral method is to approximate the above equations by

$$\tilde{C}^{n+1}(\mathbf{k},t) = \tilde{C}^n(\mathbf{k},t) + \triangle t[-k^2\{-C + C^3\}^n_{\mathbf{k}} - \kappa k^4 \tilde{C}^n(\mathbf{k},t)] \tag{12}$$

This scheme has been extensively used in numerical simulation of systems involving long-range interactions such as long-range elastic and coulombic interactions for which analytical expressions exist in Fourier space (see [16, 17]). Unfortunately, although this scheme provides excellent spatial accuracy, it is only first-order accurate in time and suffers from the same very restrictive time step constraint.

To remove the shortcoming with the small time step size associated with the explicit Euler scheme, we proposed to treat the linear fourth-order operators implicitly and the nonlinear terms explicitly. If we write the bulk driving force term $-C + C^3$ as $f(C)$, the resulted first-order semi-implicit Fourier-spectral scheme is

$$(1 + \Delta t k^4)\tilde{C}^{n+1}(\mathbf{k}) = \tilde{C}^n(\mathbf{k}) - \Delta t k^2 \{\tilde{f}(C^n)\}_{\mathbf{k}} \tag{13}$$

The accuracy in time can be improved by using higher-order semi-implicit schemes. For instance, a second-order backward difference (BDF) for $\frac{\partial \tilde{C}}{\partial t}$ and a second-order Adams-Bashforth (AB) for the explicit treatment of nonlinear term applied to (11) lead to the following second-order BDF/AB scheme:

$$\begin{aligned}(3 + 2\Delta t k^4)\tilde{C}^{n+1}(\boldsymbol{k}) =& 4\tilde{C}^n(\boldsymbol{k}) - \tilde{C}^{n-1}(\boldsymbol{k}) \\ & - 2\Delta t k^2 \left[2\{\tilde{f}(C^n)\}_{\boldsymbol{k}} - \{\tilde{f}(C^{n-1})\}_{\boldsymbol{k}}\right].\end{aligned} \tag{14}$$

We may use (13) to compute $\tilde{C}^1$, and hence $\tilde{f}(C^1)$, which are needed to start the iteration in (14). Compared with the usual finite-difference method, the Fourier-spectral method can solve the elliptic problem more efficiently and accurately [10]. The semi-implicit treatment in time enables us to use considerably larger time step size. Our preliminary numerical simulations indicate that the time step in a semi-implicit method can be two orders of magnitude larger than that in an explicit method .

3.2 Cahn-Hilliard Equation with a Variable Mobility

In the modified Cahn-Hilliard-Cook equation with a variable mobility, it is not convenient to accurately discretize the gradient operator and divergence operator by using finite difference method. However, Fourier spectral method allows us to numerically solve equation (10) without much more difficulty than the case with a constant mobility. The Fourier form of equation (10) is

$$\frac{\partial \tilde{C}(\mathbf{k}, t)}{\partial t} = i\mathbf{k} \cdot \{(1 - aC^2)[i\mathbf{k}'(\{-C + C^3\}_{\mathbf{k}'} + \kappa k'^2 \tilde{C}(\mathbf{k}', t))]_{\mathbf{r}}\}_{\mathbf{k}} \tag{15}$$

The $[\cdot]_r$ represents the inverse Fourier transform from the Fourier space to real space. The explicit Euler Fourier-spectral treatment of the above equation is

$$\frac{\tilde{C}^{n+1}(\mathbf{k}, t) - \tilde{C}^n(\mathbf{k}, t)}{\triangle t} = i\mathbf{k} \cdot \{(1 - aC^2)[i\mathbf{k}'(\{-C + C^3\}^n_{\mathbf{k}'} + \kappa k'^2 \tilde{C}^n(\mathbf{k}', t))]_{\mathbf{r}}\}_{\mathbf{k}} \tag{16}$$

However, the above scheme has a very severe time step constraint of the form

$$\Delta t \kappa K^4 \lesssim 1, \tag{17}$$

where K is the number of Fourier modes in each direction. To alleviate this constraint, we consider a semi-implicit treatment for the above equation. The idea is to split the variable mobility $(1 - aC^2)$ into A and $a(1 - aC^2) - A$, where A is a suitable constant, and treat them separately. More precisely, we add the term $A\kappa k^4 \tilde{C}^{n+1}(\mathbf{k}, t)$ to the left-hand side of (16) and $A\kappa k^4 \tilde{C}^n(\mathbf{k}, t)$ to the right-hand side of (16) to obtain

$$\begin{aligned}(1 + A\triangle t \kappa k^4)\tilde{C}^{n+1}(\mathbf{k}, t) &= (1 + A\triangle t \kappa k^4)\tilde{C}^n(\mathbf{k}, t) \\ &+ \triangle t i\mathbf{k} \cdot \{(1 - aC^2)[i\mathbf{k}'(\{-C + C^3\}^n_{\mathbf{k}'} + \kappa k'^2 \tilde{C}^n(\mathbf{k}', t))]_{\mathbf{r}}\}_{\mathbf{k}}\end{aligned} \tag{18}$$

If we choose $A = \frac{1}{2}[\max(1 - aC^2) + \min(1 - aC^2)]$, then, we have

$$|(1 - aC^2) - A| \leq A.$$

Therefore, we can expect that the time step constraint of the form (17) is no longer necessary. In practice, it is found that $A = \frac{1}{2}$ is a good approximation to $\frac{1}{2}[\max(1 - aC^2) + \min(1 - aC^2)]$. Hence, the scheme (18) is only slightly more expensive than (16) while the time step constraint is greatly alleviated. A second-order variant of (18) can also be constructed accordingly.

Our numerical study showed that such semi-implicit treatment of the variable mobility Cahn-Hilliard equation made it possible to use large time steps without losing stability and accuracy. Consequently, we can perform long-time simulations with large system sizes using Cahn-Hilliard equation with a variable mobility.

4 Computer Simulation

Our simulations were performed on a square domain discretized using lattice of 1024X1024 grid points. Periodic boundary conditions were employed. The overall scaled composition variable is zero (which corresponds to real composition of 0.5 or critical composition). The system was initially prepared in a homogeneous state by assigning a random number to each lattice site. The random numbers were uniformly distributed between 0.1 and -0.1 as the initial condition, corresponding to a high temperature initial state where the composition deviation from the average value is only caused by fluctuations. The structure function, the scaling function, the pair correlation function and the typical length scale, which were often used to characterize the dynamical system, were calculated after selected time steps. Averages were performed over 4 simulation runs using a different set of random numbers for each initial state. The discretizing grid size is chosen to be 1.0 and the time step $\triangle t$ is 1.0. For the same parameters for the local free energy and spatial grid size, an explicit scheme will require a time step size which is more than two orders of magnitude smaller than 1.0, and much smaller than the dynamic time scale of the Cahn-Hilliard equation. The Cahn-Hilliard equation with a variable mobility was computationally a factor of about 2.7 slower than Cahn-Hilliard equation with a constant mobility because extra computation time is needed to do the extra Fourier transforms in equation (18). Furthermore, since the growth rate is much slower when the coarsening process is interface diffusion controlled, longer times were needed to reach the scaling regime.

4.1 MORPHOLOGICAL EVOLUTION

Figure 1 and 2 showed typical examples of temporal evolution of morphological patterns during spinodal decomposition and subsequent coarsening for bulk diffusion controlled dynamics and for interface diffusion controlled dynamics respectively by using the same initial condition. The gray-levels represent the local compositions, with white representing high values and black representing low values. For this critical composition, there is symmetry between the two phases forming interconnected domains. Shortly after the quench, there are well defined interfaces separating regions of different phases. Domain coarsening is evident in both cases. As expected, the interface diffusion controlled coarsening evolves much slower. However, if we compare patterns with the same representative length scale, the patterns are similar.

4.2 DYNAMIC SCALING

The morphology at late times is statistically independent of time if all lengths are rescaled by a single characteristic length scale $R(t)$. That is, if we take the morphology at later times in figure 1 (or figure 2) and shrink it by an appropriate factor, it would look statistically the same as the microstructure at earlier times. This characteristic length, which represents the typical domain size, increases with time. The feature we are interested in is the scaling behavior of the pair correlation function and the structure function.

It has been shown [2] that a two-phase morphology during coarsening can be characterized by a time-dependent structure function $S(\mathbf{k}, t)$

$$S(\mathbf{k}, t) = \frac{1}{N} \langle \sum_{\mathbf{r}} \sum_{\mathbf{r}'} e^{-i\mathbf{k}\cdot\mathbf{r}} [C(\mathbf{r}+\mathbf{r}', t)C(\mathbf{r}', t) - < C >^2] \rangle \tag{19}$$

Where both sums run over the lattice L and $N = L^2$ is the total number of points in the lattice. Assuming the evolution to be isotropic, we compute the circularly averaged structure function $S(k, t)$. The normalized structure function $s(k, t)$ is defined as

$$s(k, t) = \frac{S(k, t)}{N[< C^2(\mathbf{r}) > - < C >^2]} \tag{20}$$

Where <> denotes averaging over all lattice points.

Figure 3 shows an example of the normalized and circularly averaged structure function $s(k,t)$ at 8 different time steps for interface diffusion controlled dynamics. The lines are spline fits to the simulation data. As expected, as time increases, the maximum value of the structure function increases and shifts to lower k, indicating an increase in the real-space average length scale.

Correlations of fluctuations about C were examined through the radial pair correlation function. The pair correlation function was defined by

$$G(\mathbf{r},t) = \sum_{\mathbf{k}} e^{-i\mathbf{k}\cdot\mathbf{r}} S(\mathbf{k},t) \tag{21}$$

We also consider a circularly averaged pair correlation function $G(r,t)$ and normalized pair correlation function $g(r,t)$. A main feature of the dynamical scaling is that the pair correlation function $g(r,t)$ and the structure function $s(k,t)$ depend on time through the typical length scale $R(t)$ only,

$$g(r,t) = \mathcal{G}(r/R(t)) \tag{22}$$

and

$$s(k,t) = R(t)^d \mathcal{F}(kR(t)) \tag{23}$$

where d is the dimensionality of the system and the functions $\mathcal{G}(\rho)$ and $\mathcal{F}(x)$ are the time-independent scaling functions of the system.

There are several ways to characterize the typical length scale $R(t)$, such as $k_m(t)$, the location of the maximum of $s(k,t)$ and $k_1(t)$, the first moment of $s(k,t)$ defined by

$$k_1(t) = \frac{\sum k s(k,t)}{\sum s(k,t)} \tag{24}$$

In our study we did not use $k_m(t)$ because the discrete nature of the lattice in numerical studies usually makes it difficult to determine k_m precisely. The location of the first zero of the real-space correlation function, R_g, is also a good measure of the average domain size. We compute this length by a linear interpolation of the two points closest to the first sign change in $g(r,t)$. Here we use the reciprocal of the first moment $1/k_1$ as the typical length scale. With this definition, the scaling function is $\mathcal{F}(k/k_1,t)={k_1}^2(t)s(k,t)$ for 2D. If the structure function does indeed scale, then we expect $\mathcal{F}(k/k_1,t)=\mathcal{F}(k/k_1)$.

In figure 4 we have plotted the scaling function ${k_1}^2(t)s(k,t)$ as a function of k/k_1 for different times. Figure 4a is for bulk diffusion controlled coarsening and figure 4b is for interface diffusion controlled coarsening. In the scaling regime this should be a universal curve. Data were obtained from six different times 20000,22000,24000,26000,28000,30000. They can be seen to lie on a smooth master curve, indicating that the scaling regime has been attained for both cases. The system for bulk diffusion controlled coarsening will reach the scaling regime earlier than that for interface diffusion controlled coarsening because of its faster dynamics. It is interesting to note that the scaling functions of figure 4a and 4b are quite similar although they are obtained from quite different dynamics.

We made a comparison of the circularly averaged pair correlation function for bulk diffusion controlled dynamics and interface diffusion controlled dynamics after the dynamical scaling was obeyed(t>20000). As is shown in figure 5a and figure 5b, this function exhibits characteristic oscillations about zero, which reflects the composition domain structure. From the figures we can also see the shapes of the curves are rather similar in spite of their different dynamics.

4.3 GROWTH LAW

Another important consequence of the dynamical scaling is that the characteristic domain size $R(t)$ [given by either $1/k_1(t)$ or $R_g(t)$] grows as a power law in time when the true regime is reached.

$$\overline{R(t)}^n - {R_0}^n = Kt \tag{25}$$

where $\overline{R(t)}$ is the typical domain size at a given time t ,R_0 is the initial length scale at t=0, and K is the rate for coarsening.

The rate of domain growth depends on the actual coarsening mechanism. Most authors find that for Cahn-Hilliard equation described dynamics, the growth exponent n=3. This exponent is the well-known Lifshitz-Slyozov law, which was originally derived from an evaporation-condensation mechanism for the growth of over-critical droplets in nucleation processes. It also holds for the spinodal decomposition process and its late-stage coarsening. Figure 6 shows the time dependence of domain length characterized by R_g (figure 6a) and $1/k_1$ (figure 6b) for bulk diffusion controlled dynamics. A cubic growth law is observed. One can also write the time dependence of domain size as $R(t) = A + Bt^m$. We have analyzed our data by this nonlinear fitting and found $m = 0.333 \pm 0.004$.

The cubic growth law is thought to be due to long-range diffusion through the bulk. It can be expected the coarsening will be slower through interface diffusion mechanism because the bulk diffusion is severely decreased, which may lead to a larger n in equation(15). In figure 7 we show a plot for the measure of the domain size (plot as the R_g^4 and $(1/k_1)^4$) vs. time for interface diffusion coarsening. The data can be fitted as a straight line, implying that the growth exponent n is 4 in this case. By doing the nonlinear fitting of the form $R(t) = A + Bt^m$, the exponent m we get is about 0.247 ± 0.002, which is very close to $\frac{1}{4}$.

Discussion

From our observation of the scaling function and the pair correlation function of the coarsening system, both bulk diffusion controlled coarsening and interface diffusion controlled coarsening showed very similar scaling behavior. By varying a in the variable mobility Cahn-Hilliard equation, it is possible for us to study the role of bulk diffusion in the asymptotic ordering process. According to our results, the scaling function is independent of a, i.e., the scaling behavior does not depend on the detailed dynamics. Lacasta et al. [6] found this seems to be true also for the off-critical quenching with different volume fraction of the two phases. Furthermore, it may indicate that there is some universal form for phase separation processes.

The growth law merits some comments because it is very important to understand the kinetics of the late stage coarsening. The dynamical exponents m in $R(t) = A + Bt^m$ for different mechanisms have been noted by Furukawa et al.[18]. For diffusion through the bulk, the coarsening mechanism was thought to be evaporation-condensation. Material diffuses from surfaces of high curvature to surfaces of low curvature. This can be understood as a curvature driven process which gives a dynamical exponent m of $\frac{1}{3}$. For diffusion along interfaces, inhomogeneous composition profiles on interface are smooth out by diffusion. The corresponding exponent m would be $\frac{1}{4}$. Our simulations on large system size and long times have confirmed the above results. Yeung et al. [7] also found the growth law of $R(t) \sim t^{1/4}$ when diffusion is only through the interface. The exponent m Lacasta obtained for interface diffusion coarsening is 0.22 ± 0.01[5], below the predicted value $\frac{1}{4}$.

Changing a in the Cahn-Hilliard equation with variable mobility will affect the growth rate greatly. When a is in the range of 0$\sim$1, the coarsening mechanism contains both bulk and interfacial diffusion. The growth exponent m can be expected between $\frac{1}{3}$ and $\frac{1}{4}$, depending on which mechanism is dominant. For example, if a=0.9, we fit the data by the form $R(t) = A + Bt^m$ and get an approximate exponent of m=0.30. For intermediate values of a , it was mentioned by Lacasta et al. that there was a crossover behavior of the growth law[5]. They gave a qualitative estimation of the crossover through the introduction of a critical characteristic domain size. It was expected the cubic growth law (n=3) would dominate for very long times because bulk diffusion will dominate the late stage of coarsening, recovering the ordinary Cahn-Hilliard like behavior. Bray et al. derived the a more general growth law when the minority phase occupies an infinitesimal volume fraction[8]. Instead of writing the diffusion coefficient in the form of $(1 - aC^2)$, Bray et al. use $(1 - C^2)^\alpha$ as the diffusion coefficient. They derived the a expression of the growth exponent $R(t) \sim t^{(1+\alpha)}$.

For bulk diffusion controlled dynamics, it is usually accepted that the noise term does not affect some important features of the late stages of evolution (such as the growth law for the characteristic domain size and the scaling functions) for spinodal composition. However, Yeung et al. believed that noise might be

more important in interface diffusion controlled dynamics[7]. Noise may affect the mobility, leading to a faster rate of growth. The effect of noise term on the kinetics of coarsening through both bulk diffusion and interfacial diffusion remains a topic for us to carry out large scale and long time simulations.

Conclusion

In this paper, an efficient and accurate numerical scheme, the Semi-implicit Fourier-Spectral Method, was proposed for solving the Cahn-Hilliard equation with a variable mobility. Compared with the conventional forward Euler finite-difference method, it is orders of magnitude more efficient and accurate, thus allowing us to work on large systems and for long times. We have studied the coarsening kinetics of an interconnected two phase microstructure from the Cahn-Hilliard equation with a compositional dependent mobility. Particularly we compared the kinetics of bulk-diffusion-controlled coarsening and interface-diffusion-controlled coarsening. It was shown that the morphological pattern evolution in the interface-diffusion-controlled coarsening is much slower than that in the bulk-diffusion-controlled coarsening. However, in spite of their quite different dynamics, the scaling behavior for the coarsened microstructure characterized by the scaling function and pair correlation function looks quite similar. Finally we have also studied the growth law for the characteristic domain size which can be characterized by either the inverse of the first moment $k_1(t)$ or the location of the first zero of the real-space correlation function $R_g(t)$. Our analysis showed that a cubic growth law $\bar{R}^3 \sim t$ was obeyed in the scaling regime for the bulk diffusion controlled coarsening, while a fourth power growth law $\bar{R}^4 \sim t$ was observed for interface diffusion controlled coarsening.

Acknowledgments

The authors are grateful for the financial support from the Sandia National Laboratory and the National Science Foundation under DMR 96-33719 and DMS 9721413. The simulation was performed at the San Diego Supercomputer Center and the Pittsburgh Supercomputer Center.

References

[1] L.Q. Chen, Y.Z. Wang. Continuum field approach to modeling microstructural Evolution, JOM 48 (1996) 13-18

[2] A. Chakrabarti, R. Toral and J.D. Gunton, Late-stage coarsening for off-critical quenches: Scaling functions and the growth law, Physical Review E 47(1993) 3025-3038

[3] T.M. Rogers and R.C. Desai, Numerical study of late stage coarsening for off-critical quenches in the Cahn-Hilliard equation of Phase separation, Phys. Rev. B. 39(1989) 11956-11963

[4] T. Küpper and N. Masbaum, Simulation of particle growth and ostwald ripening via the Cahn-Hilliard equations, Acta Metall. Mater. 42(1994) 1847-1858

[5] A.M. Lacasta, A. Hernández-Machado, J.M. Sancho and R. Toral. Domain growth in binary mixtures at low temperatures, Physical Review B 45 (1992) 5276-5281

[6] A.M. Lacasta, J.M. Sancho, A. Hernández-Machado and R. Toral. Effects of domain morphology in phase-separation dynamics at low temperature, Physical Review B 48 (1993) 6854-6857

[7] C. Yeung, Ph.D. thesis, Some problems on spatial patterns in nonequilibrium systems, Univeristy of Illinois, 1989

[8] A.J. Bray and C.L. Emmott, Lifshitz-Slyozov scaling for late-stage coarsening with an order-parameter-dependent mobility, Physical Review B 52(1995)R685-R688

[9] L.Q. Chen, J. Shen. Applications of semi-implicit Fourier-spectral method to phase field equations, Computer Physics Communications 108 (1998) 147-158

[10] C. Canuto, M.Y. Hussaini, A. Quarteroni and T.A. Zang, in Spectral Methods in Fluid Dynamics, edited by R.Glowinski et al., Springer Series in Computational Physics (Springer-Verlag, Berlin, 1987)

[11] Y. Oono, Structural stability of spinodal decomposition, in: Mathematics of Microstructure Evolution, EMPMD Monograph Series 4, L.Q.Chen, B. Fultz, J.W. Cahn, J.R. Manning, J.E. Morraland, J.A. Simmons, eds. (TMS, SIAM, Philadelphia, PA, 1996) pp.355-365

[12] J.W. Cahn and J.E. Hilliard, Free energy of a nonuniform system I. Interfacial free energy, Journal of Chemical Physics 28(1958) 258-267

[13] H.E. Cook, Brownian Motion in spinodal decomposition, Acta Metall. 18(1970) 297-306

[14] J.S. Langer, M. Bar-on and H.D. Miller. New computational method in the theory of spinodal decomposition, Physical Review A 11(1975) 1417-1429

[15] K. Kitahara and M. Imada, On the kinetic equations for binary mixtures, Supplement of the Progress of Theoretical Physics 64(1978) 65-73

[16] Y. Wang, L.Q. Chen and A.G. Khachaturyan, Kinetics of strain induced morphological transformation cubic alloys with a miscibility gap, Acta Metall. Mater. 41(1995) 279-296

[17] D.N. Fan and L.Q. Chen, Possibility of spinodal decomposition in yittria-partially stablized zirconia($ZrO_2 - Y_2O_3$) system - a theoretical investigation, J. Am. Ceram. Soc. 78(1995) 1680-1686

[18] H. Furukawa, A dynamic scaling assumption for phase separation, Advances in Physics, 34 (1985)703-750

List of Figures

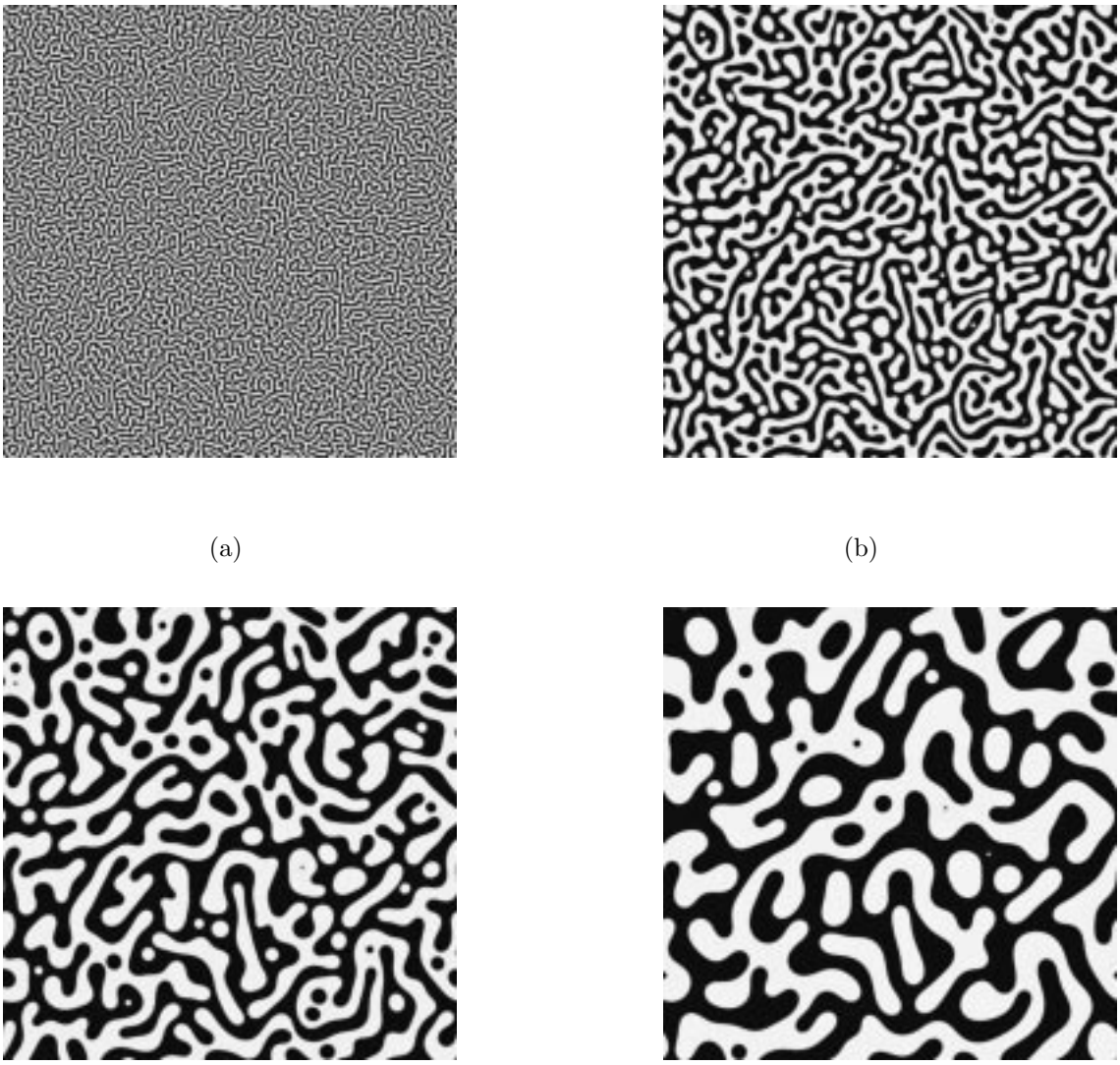

(a) (b)

(c) (d)

Figure 1: Morphological patterns during spinodal decomposition and subsequent coarsening for bulk diffusion controlled dynamics: (a) t=100, (b) t=2000, (c) t=10000, (d) t=30000

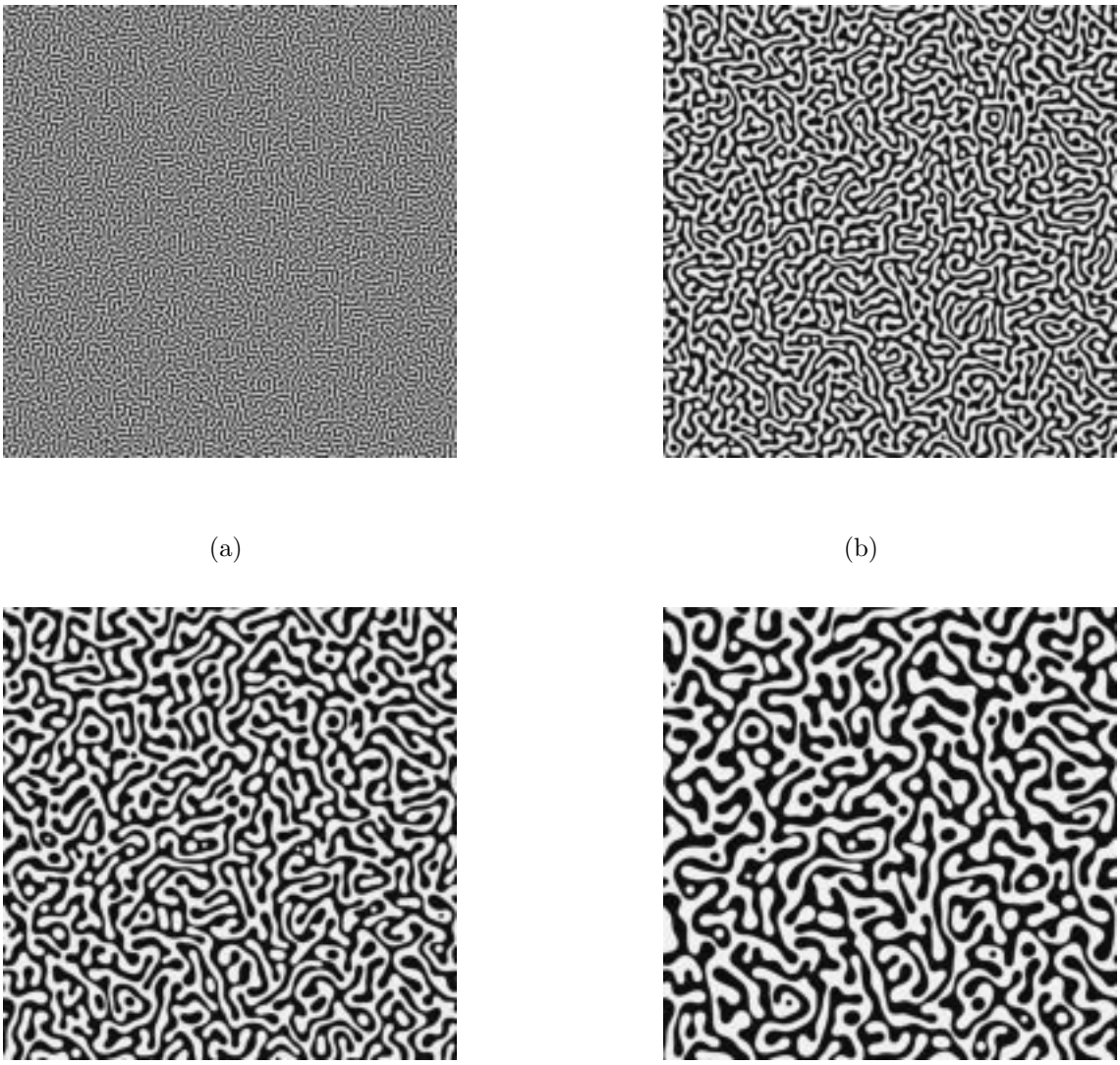

(a) (b)

(c) (d)

Figure 2: Morphological patterns during spinodal decomposition and subsequent coarsening for interfacial diffusion controlled dynamics: (a) t=100, (b) t=2000, (c) t=10000, (d) t=30000

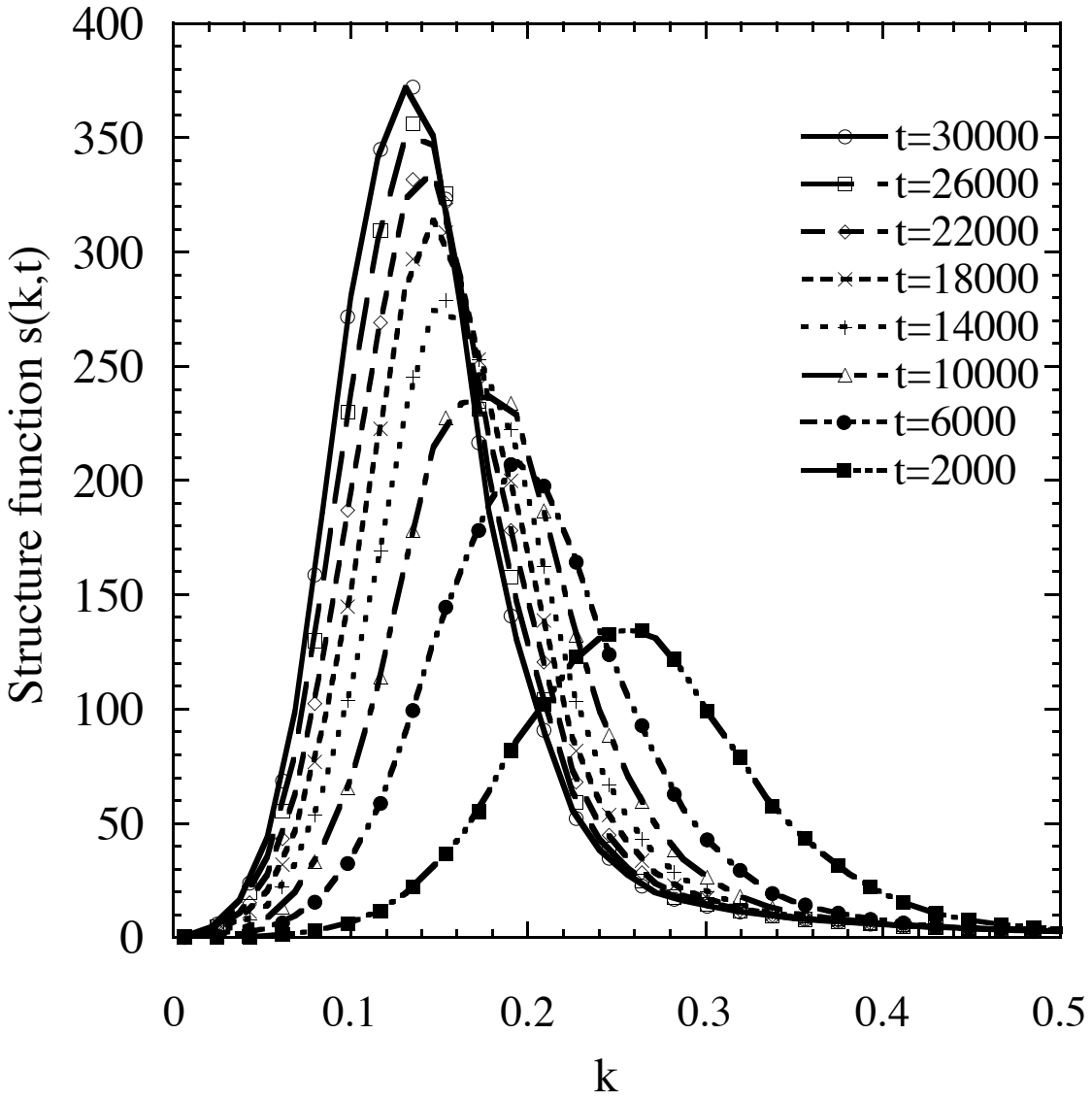

Figure 3: Structure function as a function of k at 8 different time steps for interface diffusion controlled coarsening

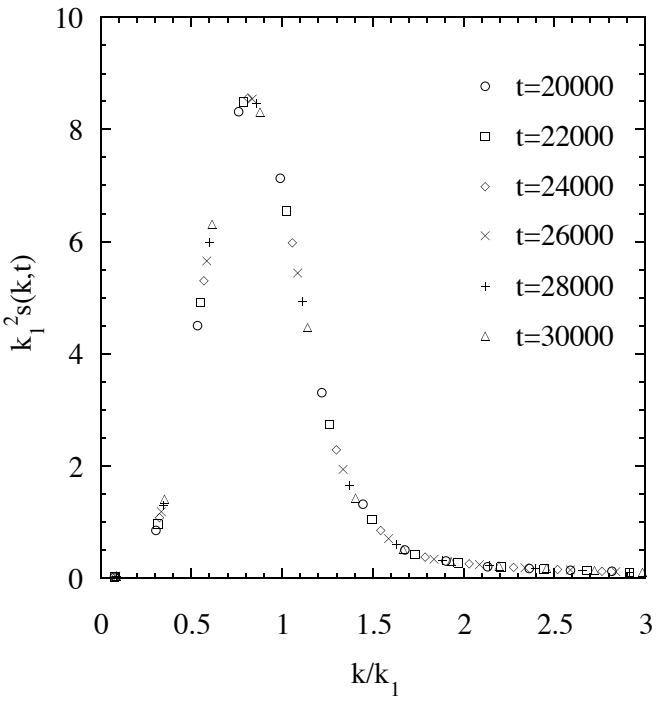

(fig.4a)

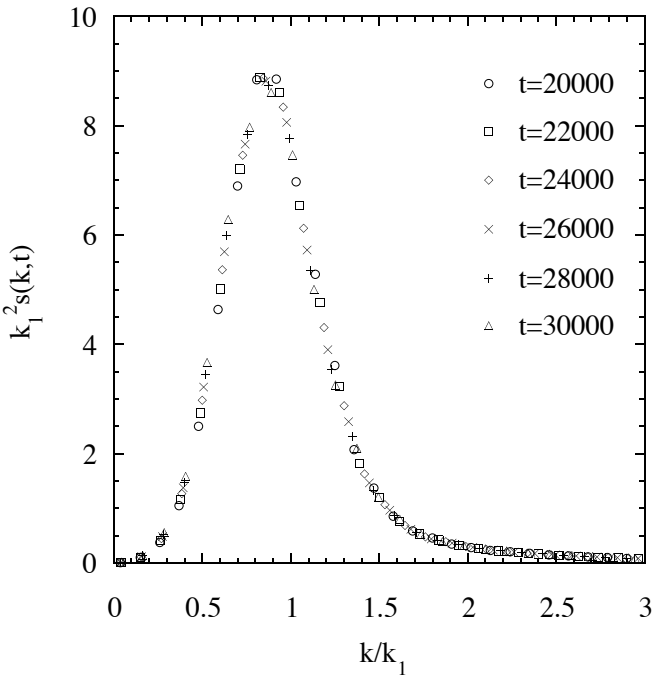

(fig.4b)

Figure 4: Scaling function as a function of k/k_1 from 6 time steps at late stage of coarsening: fig. 4a for bulk diffusion controlled dynamics; fig. 4b for interface diffusion controlled dynamics

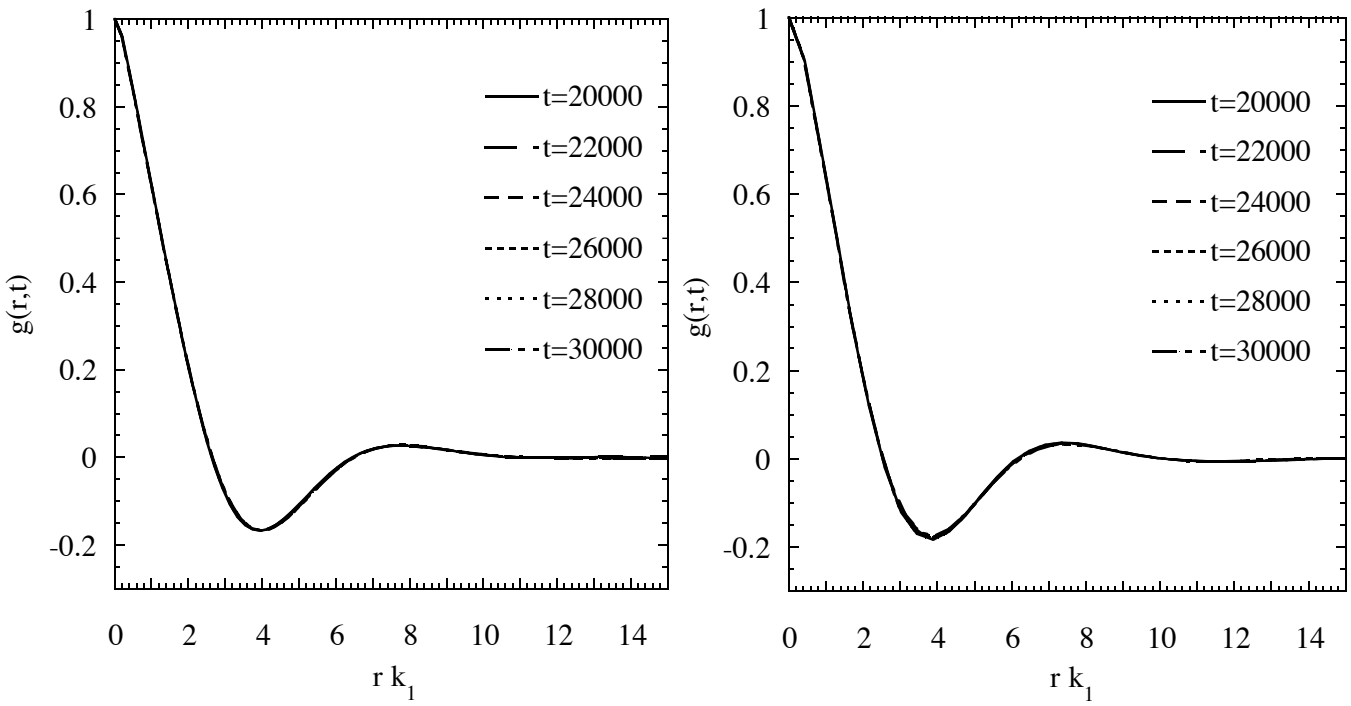

(fig.5a) (fig.5b)

Figure 5: Plot of the normalized pair correlation function g(r,t) vs $r \cdot k_1$: fig. 5a for bulk diffusion controlled dynamics; fig. 5b for interface diffusion controlled dynamics

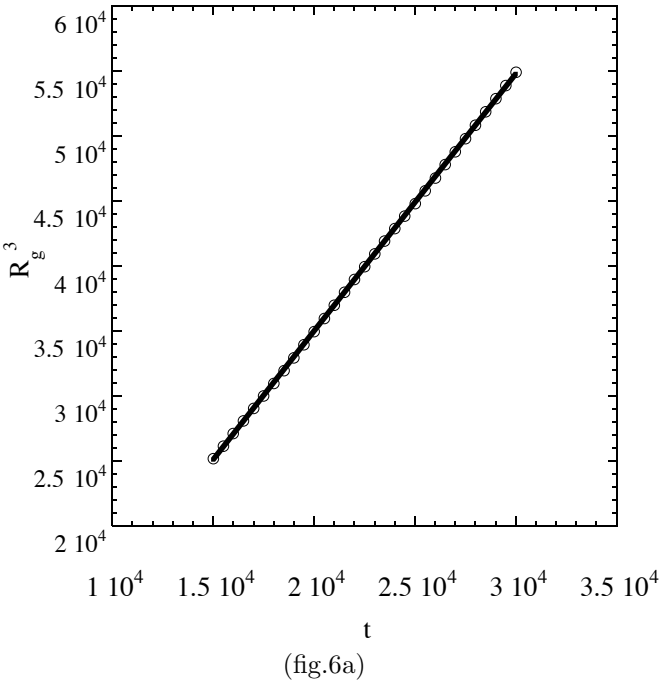

(fig.6a)

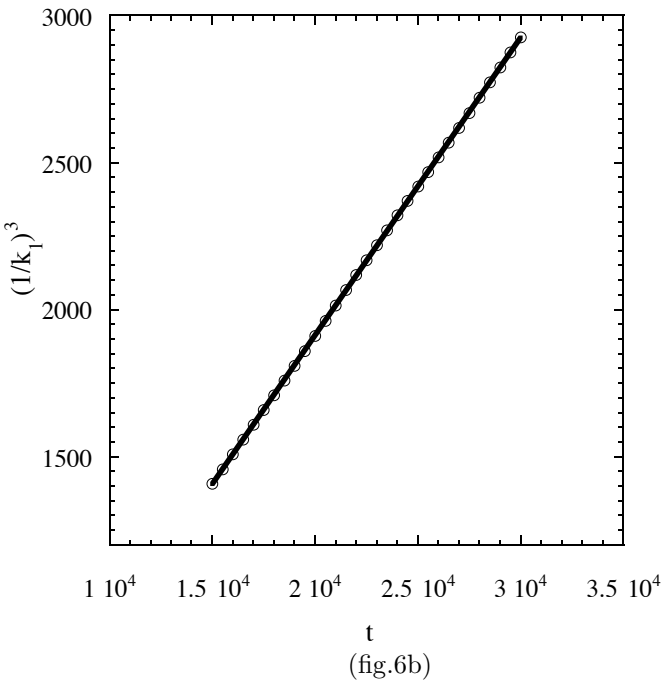

(fig.6b)

Figure 6: The cubic of the average domain size vs time at the late stage of bulk diffusion coarsening: Fig. 6a domain size characterized by R_g; Fig. 6b domain size characterized by $(1/k_1)$

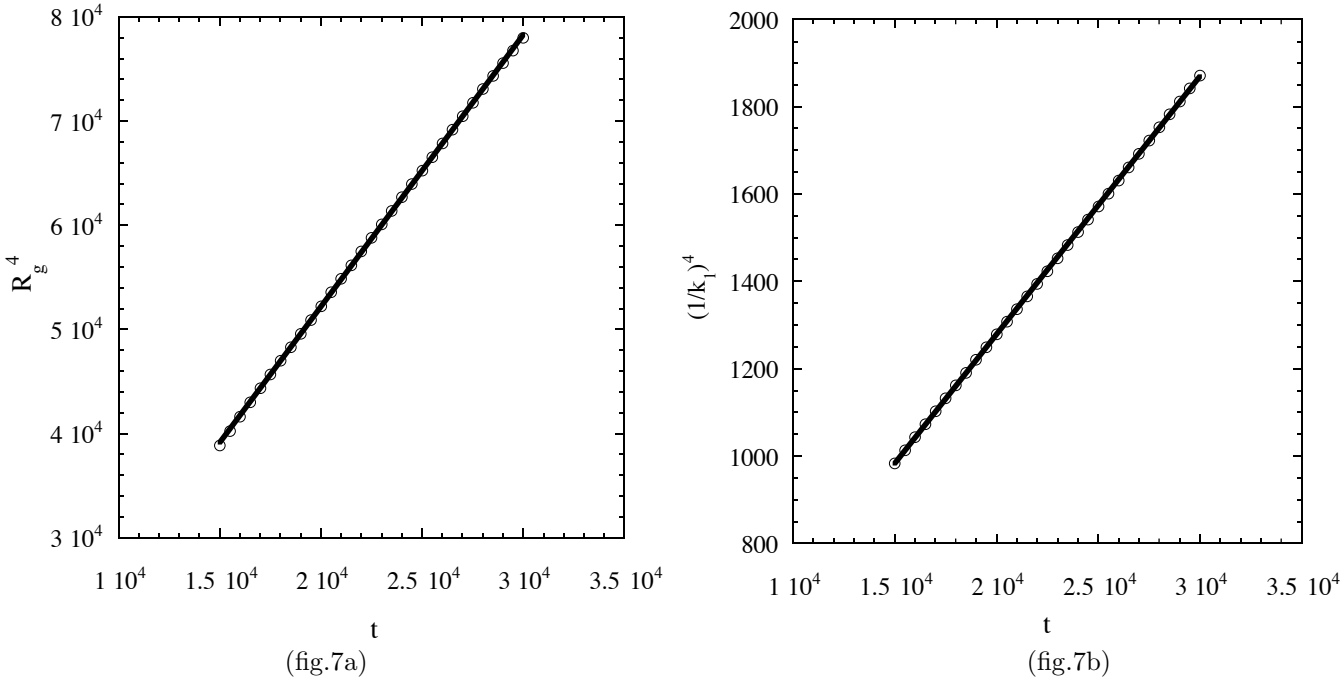

(fig.7a) (fig.7b)

Figure 7: The fourth power of the average domain size vs time at the late stage of bulk diffusion coarsening Fig. 7a domain size characterized by R_g; fig. 7b domain size characterized by $(1/k_1)$